International Journal of Innovative Computing, Information and Control
Volume **20**, Number **4**, August **2024**

ICIC International ©2024 ISSN 1349-4198
pp. **1199–1214**

BUNGEE CORD-BASED UNMANNED AERIAL VEHICLE (UAV) LAUNCHER WITH TRAJECTORY PREDICTION

Ronny Mardiyanto, Devy Kuswidiastuti, Ruth Johana Hutagalung
Ahmad Fauzi Aulia and Pradhipta Dwi Nugroho

Department of Electrical Engineering
Institut Teknologi Sepuluh Nopember
Kampus ITS, Sukolilo, Surabaya 60111, Indonesia
{ rony; devy }@ee.its.ac.id; ruth.205022@mhs.its.ac.id; ahmad.f.aulia@sat.co.id
n.pradhipta@gmail.com

Received September 2023; revised January 2024

Abstract. *Many UAVs fail to take off because of launchers with poor trajectory prediction. Moreover, the cost of manufacturing launchers remains prohibitively high for developing countries seeking to advance their UAV capabilities. In this paper, we propose a low-cost bungee cord-based UAV launcher that provides trajectory prediction and the ability to read the wing area of the UAV to be flown, thereby enhancing the success rate of UAVs to takeoff. The designed launcher features an adjustable angle and can be controlled remotely. The wing area reading was obtained through computer vision using a camera placed on the top of the UAV. The testing results indicate a trajectory difference of 0.14 m between the simulation result and the actual flight. This shows that the proposed launcher significantly improves the accuracy of UAV takeoffs.*
Keywords: Bungee cord, Launcher, Trajectory, UAV

1. **Introduction.** Over the last decade, the use of Unmanned Aerial Vehicles (UAVs) has significantly expanded, impacting diverse fields. UAV technology has been adopted in military applications [1-3], agriculture [4], environmental and healthcare [5], and various other areas [6-8]. Several UAVs have been integrated with IoT and radar systems for surveillance and monitoring systems in a geographic area for security [1]. Each UAV is equipped with GPS and GSM modules to accurately track the location of each UAV and facilitate communication between the UAVs and the control unit through the Internet network. The information generated by each UAV is transmitted to the control unit through data transmission and stored in a database using Internet of Things (IoT) based devices. [4] focuses on discovering optimal algorithms that organize minimal routes to be taken by the UAV system to distribute medicine to all infected areas in the agricultural environment. The algorithms are designed to overcome non-convex obstacles, involve pest-free zones, and avoid areas infested by pests. An IoT-based architecture with the assistance of UAVs to monitor air quality was developed [5]. Toxic gas sensors are installed in an integrated array on the UAV to enhance data monitoring accuracy and localization. The hub module uses the MSP430 microcontroller to facilitate communication between the airborne sensors on the drone using the nRF24L01 communication module. Cloud facilities are implemented through the Amazon Web Services Elastic Computing (AWS EC2) Instance as the platform for data storage and processing. In addition, a Graphical User Interface (GUI) is designed to enable real-time sensor data monitoring from the UAV. Although UAV technology has been established very well, a challenge still exists

DOI: 10.24507/ijicic.20.04.1199

on how to make it low cost and safe. This paper focuses on how to make a UAV take off accurately and safely by developing a launcher.

The initial flight and landing stages [9] are the most challenging and critical phases in UAV missions, even though they account for only approximately 6% of the total flight time. Approximately 53% of the incidents occurred during these stages among the missions conducted. This poses a significant problem for UAVs in achieving precise, autonomous, and safe takeoffs in environments with varying conditions [10]. Accurate control during the takeoff and landing phases is necessary to ensure the safety of the entire flight. [11] discusses the development of software for UAV monitoring during takeoff and landing using Microsoft Visual C++ 6.0 and virtual instruments. One of the aims of this paper is to develop a trajectory prediction for a specific type of UAV takeoff. Several modern UAVs are specifically designed for takeoff using launchers [12-14]. There are five common launcher systems used to launch UAVs: pneumatic [15], hydraulic, bungee cord [10,13,14], kinetic energy [16], and Rocket-Assisted Takeoff (RATO). Other launcher systems include electromagnetic [12,17,18] and spring-driven [19]. [15] describes the constitution, structure, working principles, and launch process of the wedge-shaped pneumatic launcher used for several UAVs. The physical model of the launcher is simplified, and two dynamic models of each UAV launcher system are constructed using Lagrange equations and MSC.ADAMS software. By analyzing these models, the acceleration and velocity curves of the UAV over time are obtained. To validate the accuracy of these models, the simulation results are compared with the experimental data. Furthermore, research has been conducted on various parameters that increase the success rate of UAV launches and optimize the system. Optimization efforts reduce maximum load and acceleration fluctuations. A kinetic energy launcher with stored energy in a rotating wheel driven by an electric motor was developed [17]. By employing a transmission system, controlled coupling, and electromagnetic brake, the speed and acceleration of the launched object can be precisely controlled. This paper presents and discusses the dynamic equations, simulation results obtained using MATLAB/Simulink software, and a conceptual CAD model of the preliminary engineering solution for the kinetic UAV launcher. Integration of the advantages of UAV and electromagnetic launch technologies has been developed [18]. Unmanned Aerial Vehicles (UAVs) have significant advantages in maneuverability, economic efficiency, flexible flight, and low environmental requirements. Meanwhile, electromagnetic launch technology has significant advantages such as controllable launching, precise anchor speed, clean energy, and low recoil. [19] focuses on addressing the challenges that require a large area for UAV takeoff. This research encompasses various relevant theories, including mechanical design, engineering drawings, and principles of aerodynamics. The outcome of this launcher would result in a constant force being applied to the launched UAV, thereby reducing the risk of repeatedly launching the UAV. The bungee cord UAV launcher applies the principle of converting potential energy stored in the elastic material of the bungee cord by stretching the bungee cord backward. The initial design requirements of the bungee cord launcher are tailored to the specific UAV to be launched [13]. This UAV launcher has a compact and modular design, allowing easy transportation and installation in various locations or flight facilities [20]. Compared with other launching methods, such as rocket launchers or air launchers, the bungee cord launcher offers a more financially economical and safer solution. This paper proposes a UAV launcher powered by a bungee cord. It reduces the construction cost. It will be suitable for developing countries to develop their own UAV system because our proposed launcher requires a minimum budget.

The design and development of elastic rubber-type launchers have been previously conducted in [10,13,14]. [10] focuses on developing short-range takeoff technology for small

and medium-sized UAVs. The process begins with the design of the elastic-rope launcher, which includes estimating the catapult distance based on the maximum load constraints and takeoff speed requirements. Then the next one is determining the initial length of the elastic rope according to geometric configurations and launcher deformation ratio constraints and calculate parameters using the principle of energy conservation. This is achieved by the design and experimental verification of a UAV launcher. [13] designed and tested a bungee cord UAV launcher for the LSU-02 UAV. One of the main requirements of the launcher is its ability to propel the LSU-02 with a maximum takeoff mass of 15 kg above the 7 kg cradle (total mass of 22 kg) and achieve a launch speed of 15.2 m/s at the end of the launch track. The launcher was tested to launch LSU-02 with a UAV takeoff mass of 14.4 kg and a cradle mass of 7.5 kg (total of 21.9 kg). In the testing, the launcher successfully launched LSU-02 within 0.27 s with a launch track distance of 2.5 m. Before launch, the bungee cord is stretched by a wire pulled through a roller according to the required tension level [20]. This system typically has several safety pins set before stretching and released with a trigger. It can be understood that operating a bungee cord launcher effectively requires skill and experience. Understanding how to adjust the magnitude of the bungee cord tension, determining the proper launch angle, and comprehensively managing the launch process are essential factors to achieve a successful launch. Based on the concerns above, it becomes evident that the UAV launcher system for optimizing the UAV takeoff phase is a crucial research area.

This paper proposes an automated bungee cord-type UAV launcher system and software development for predicting the UAV trajectory. The contributions of this research are as follows.

- It proposes a low-cost UAV launcher with an adjustable angle and tension that can be remotely controlled.
- The proposed method for UAV wing area prediction is based on computer vision. The wing area is used to set launcher parameters such as the angle and tension of the bungee cord. The appropriate angle and tension of the bungee cord make the UAV launch accurately and safely.
- The prediction method was implemented using a microcontroller to predict the trajectory.

The next section describes methodology, vision-based UAV wing area estimation, trajectory prediction, and results. The methodology explains the hardware design and the work flow. The vision-based UAV wing area estimation section explains how the wing area of UAV is calculated. The trajectory prediction section explains equations are used to predict the UAV trajectory. The result and discussion section presents experiment results and discussion. The manufacturing costs and its limitations are also discussed. The conclusion is drawn based on the test results and analysis.

2. Methodology.

The proposed launcher design is shown in Figure 1. The launcher requires two operators: a UAV pilot, and a UAV launcher operator. The series of components composing the main frame of the UAV launcher included the launch frame, load cell sensor mount, DC motor mount, pneumatic cylinder mount, and safety pin as the trigger. The predominant material used for the launch frame was iron metal in a box-shaped design with dimensions of 4 cm $\times$ 6 cm $\times$ 14 mm, launch angle inclination of $\pm$100 degrees, and launch plane length of $\pm$3.5 m. Y-shaped structures made of iron bars were used as couplers between the wire and bungee cords to increase the efficiency of the number of pull wires. Each side utilized two bungee cords, resulting in a total of four bungee cords used in the UAV launcher system. Cradle design involved using flat iron plates as supports to position the UAV in a ready position for takeoff. In the gap between the cradle

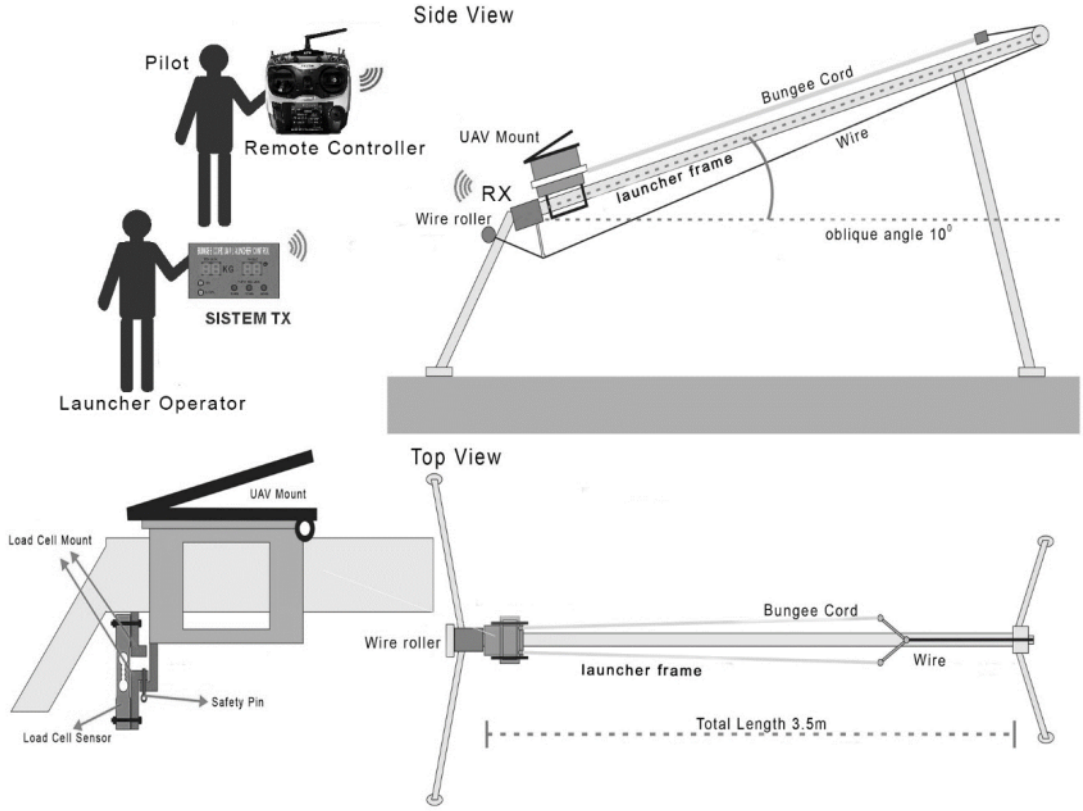

FIGURE 1. Design of the automated bungee cord-type UAV launcher system

and the launch frame, there was a bearing made of iron metal that functioned as a roller to reduce the frictional force resulting from the interaction of the two objects. The load cell sensor mount was positioned vertically on the launch frame, near the launch roller. The safety pin acts as a bridge between the load cell sensor mount and the launch roller. When the safety pin was pulled, the launch roller detach. The DC motor is positioned parallel to the wire reel on the main frame, using iron plates as the base. The DC motor and the Electronics parts were located at the legs of the main frame. The DC motor was connected to the wire reel through two gear wheels with a gear ratio of 1 : 2. As a result, the torque generated by the DC motor was doubled. The pneumatic cylinder and solenoid air valve were positioned in a crossed arrangement at the rear legs of the launch frame. The direction of the pneumatic cylinder's piston movement was directed downwards, following the direction of the safety pin's pull. The solenoid air valve was placed adjacent to the pneumatic cylinder to minimize the length of the air hose used as the actuating medium for the pneumatic cylinder's piston.

The Electronics parts consist of the receiver (RX) and transmitter (TX) subsystems. The RX is responsible for processing the data acquired from the sensors, which are then used to manipulate the actuator displacement. The TX transmits instructions to the RX to operate the actuators and display the sensor data on the RX display. The trigger system refers to the electronic device responsible for controlling the trigger used to initiate UAV launch.

In contrast to the previously proposed methods in the literature, the approach presented in this paper does not involve direct contact between the launching frame and the ground surface. The need for additional space on the lower part of the frame to accommodate peripheral electronic equipment is an argument for the update. The previous approach used a bungee cord that was not fully stretched. This transformation enhances

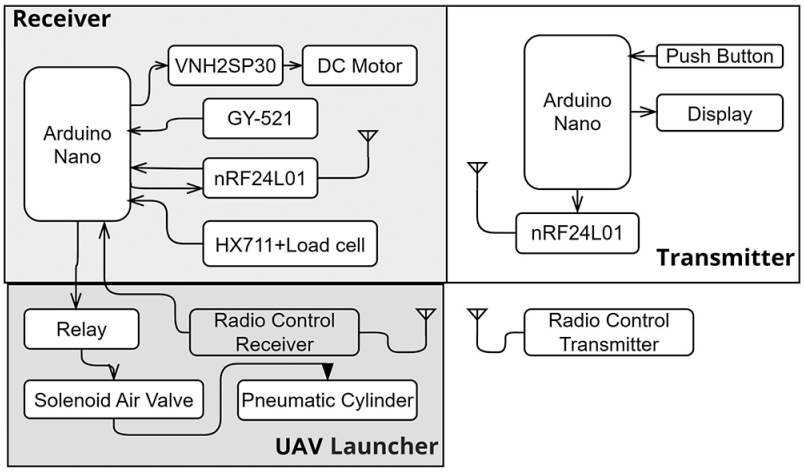

FIGURE 2. Block diagram of the bungee cord-type UAV launcher system

the efficiency of the rolling process because of the additional wire on the bungee cord. The applied bungee cord also has higher elasticity than conventional cords. A design block diagram of the proposed launcher system is shown in Figure 2.

The series of components forming the RX system comprised an Arduino Nano, a DC motor, a DC motor driver, an HX711 module, a load cell sensor, an IMU sensor (a combination of gyro and accelerometer sensors), and an nRF24L01 module. The load cell sensor transmitted the magnitude of the UAV launcher's load data to the HX711 module, which acted as an ADC module. The IMU sensor module GY-521 was positioned parallel to the launch plane to gather and transmit data about the Y-axis position of the UAV launcher frame. Arduino processed input data from the load cell sensor and IMU sensor (Inertial Measurement Unit) to control the DC motor through the DC motor driver. During the data processing stage, the Arduino Nano used the data received from the load cell and IMU sensors to perform analysis and decision-making processes. Subsequently, the Arduino Nano used this information to control the movement of the DC motor using the VNH2SP30 module. The Arduino Nano also read data from the UAV's RC receiver and controlled the relay to activate the pneumatic cylinder in the trigger system. These configurations make the proposed launcher have features of adjustable angle and can be controlled remotely.

3. **Vision-Based UAV Wing Area Estimation.** The wing area is estimated by a camera placed on the top of the UAV, which acquires three channels of UAV images (Red, Green, Blue) [R, G, B]. Due to the fact that HSV (Hue, Saturation, Value) [H, S, V] image type is robust to illumination changes, an RGB to HSV conversion is executed. Separation between the UAV wing and background applies a threshold that remains just a UAV image [H_T, S_T, V_T]. Noise and unwanted items on the image result are eliminated using morphological operations such as dilate and erode, yielding an image [H_D, S_D, V_D]. Connected component labeling was used to extract information on the number of blobs (N) and the area of each blob (A_N). Finally, the wing area is calculated by selecting the area of the largest blob. The wing area estimation method is shown in Figure 3.

4. **Trajectory Prediction.** The workflow of the proposed launcher is shown in Figure 4(a). The operator sets launcher parameter using the remote control, and then these parameters will be entered into our trajectory prediction simulation. It read wing area using scanning box, and then used it to predict the UAV trajectory during takeoff. It will decide whether the launch is safe or not. In designing the UAV trajectory prediction

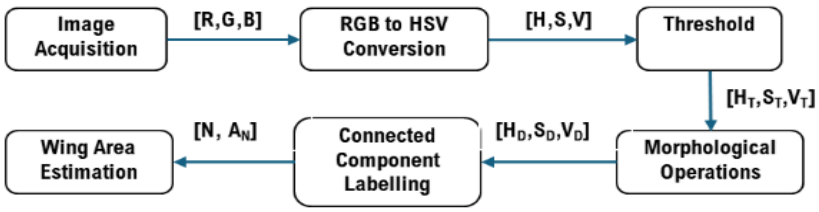

FIGURE 3. Wing area estimation

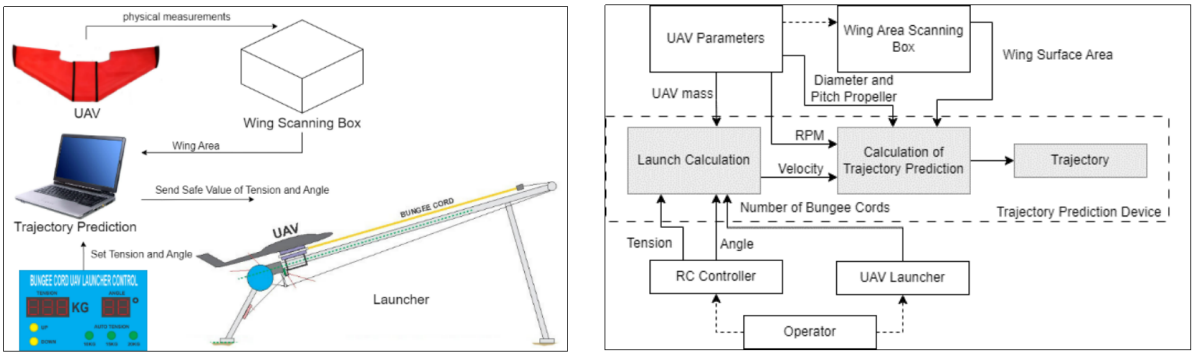

(a) (b)

FIGURE 4. The workflow of the (a) proposed UAV launcher; (b) fixed-wing UAV trajectory prediction system

system, the initial stage starts with formulating the UAV trajectory prediction formula, followed by designing the UAV trajectory prediction simulation. Figure 4(b) illustrates the series and workflow of the fixed-wing UAV trajectory prediction system. There are two main calculations performed, namely the launch calculation and the trajectory prediction calculation. The launch calculation requires inputs such as tension, launch angle, the number of bungee cords, and UAV mass.

The output of the launch calculation includes the initial velocity and the UAV's takeoff time. On the other hand, the trajectory prediction calculation requires inputs such as the diameter and pitch of the propeller, motor RPM, and the UAV's wing area. The output of the trajectory prediction calculation includes the thrust and acceleration of the UAV. The developed UAV trajectory prediction device consists of two types, a simulation that utilizes QT Creator and an Arduino-based device. The trajectory prediction simulation features two interfaces or pages. The first page presents the parameters required for performing the launch calculation. The second page performs the trajectory prediction calculation and focuses on visualizing the UAV trajectory prediction when the 'Generate' button on the first page is pressed. The Arduino-based trajectory prediction device focuses on providing information about the potential trajectory with three classification options: safe, risky, or dangerous.

In the initial condition, the object (cradle and UAV) had zero magnitude of velocity (v) and time (t). After the trigger system was activated, the cradle moved toward the end of the launcher with the final velocity (vf) and time (tf). The free-body diagram experienced by the object is visualized in Figure 5(a).

The object that satisfies Newton's Second Law is expressed in Equation (1). The forces experienced by the object are described in Equation (2). Fx represents the force exerted by the bungee cord stretching against the object. This interaction complied with Hooke's Law is expressed in Equation (3). q is the coefficient of elasticity, x_0 is the initial length

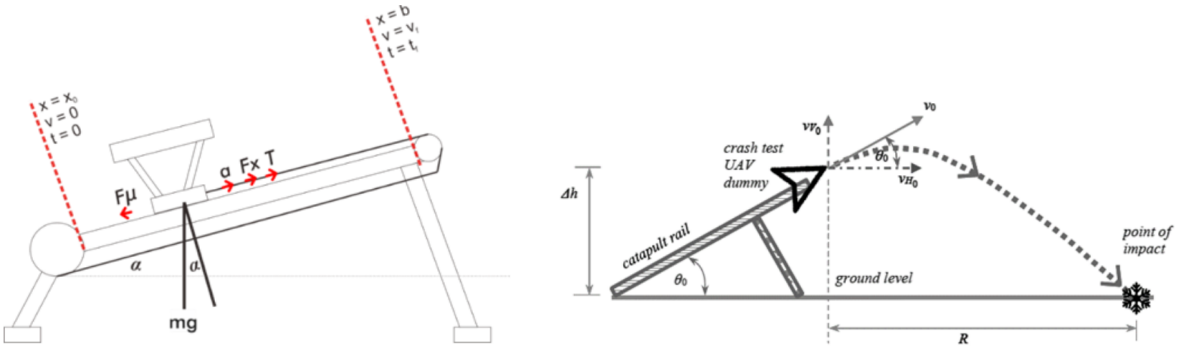

(a) Free body diagram of the UAV launcher (b) The overview of the UAV movement scheme

FIGURE 5. Free body diagram of the UAV launcher and the UAV movement scheme

of the bungee cord, and b is the final length of the bungee cord. $F\mu$ is the frictional force expressed in Equation (4). N was the normal force of the object influenced by the launch angle expressed in Equation (5). By substituting Equation (5) into Equation (4), we obtained Equation (6). By substituting Equation (3) and Equation (6) into Equation (2), we obtained Equation (7). The acceleration (a) is the second derivative of the position (x). The parameter a was substituted as x'' and grouped with the variable x. Equation (8) was divided by m to simplify the formula.

$$\sum F = ma \tag{1}$$

$$Fx - F\mu + mg\sin\alpha = ma \tag{2}$$

$$Fx = q(x_0 - b) \tag{3}$$

$$F\mu = \mu \cdot N \tag{4}$$

$$N = mg\cos\alpha \tag{5}$$

$$F\mu = \mu \cdot mg\cos\alpha \tag{6}$$

$$ma = q(x - b) + mg\mu\cos\alpha + mg\sin\alpha \tag{7}$$

$$ma = qx - qb + mg(\mu\cos\alpha + \sin\alpha) \tag{8}$$

$$mx'' - qx = -qb + mg(\mu\cos\alpha + \sin\alpha) \tag{9}$$

$$x'' - x\left(\frac{q}{m}\right) = -b\left(\frac{q}{m}\right) + g(\mu\cos\alpha + \sin\alpha) \tag{10}$$

The equation in [21] was applied because it is a nonhomogeneous second-order differential equation.

$$x(t) = \mathrm{C}_1\cos\sqrt{\frac{q}{m}}\cdot t + \mathrm{C}_2\sin\sqrt{\frac{q}{m}}\cdot t + \frac{mg}{q}(\mu\cos\alpha + \sin\alpha) + b \tag{11}$$

To obtain the values of C_1 and C_2, the initial conditions were substituted into Equation (11). At the initial condition, when $t = 0$, $x = x_0$, and $v = 0$. By substituting the initial value into Equation (11), the value of C_1 was obtained as follows:

$$x(0) = \mathrm{C}_1\cos 0 + \mathrm{C}_2\sin 0 + \frac{mg}{q}(\mu\cos\alpha + \sin\alpha) + b \tag{12}$$

$$x_0 = \mathrm{C}_1 + \frac{mg}{q}(\mu\cos\alpha + \sin\alpha) + b \rightarrow \mathrm{C}_1 = x_0 - \left[\frac{mg}{q}(\mu\cos\alpha + \sin\alpha) + b\right] \tag{13}$$

To obtain the value of C_2, the differentiation of $x(t)$ was performed such that the equation $v = 0$.

$$x'(t) = -\left[\mathrm{C}_1\sqrt{\frac{q}{m}}\sin\sqrt{\frac{q}{m}}\cdot t\right] + \left[\mathrm{C}_2\sqrt{\frac{q}{m}}\cos\sqrt{\frac{q}{m}}\cdot t\right] + 0 = 0$$

$$x'(0) = -\left[\mathrm{C}_1\sqrt{\frac{q}{m}}\sin 0\right] + \left[\mathrm{C}_2\sqrt{\frac{q}{m}}\cos 0\right] + 0$$

$$x'(0) = \mathrm{C}_2\sqrt{\frac{q}{m}} \tag{14}$$

Hence, $x'(0) = 0 \rightarrow \mathrm{C}_2 = 0$

$$x(t) = \left[x_0 - \frac{mg}{q}(\mu\cos\alpha + \sin\alpha) - b\right]\cos\sqrt{\frac{q}{m}}\cdot t + \frac{mg}{q}(\mu\cos\alpha + \sin\alpha) + b \tag{15}$$

$$x'(t) = -\left[x_0 - \frac{mg}{q}(\mu\cos\alpha + \sin\alpha) - b\right]\sqrt{\frac{q}{m}}\sin\sqrt{\frac{q}{m}}\cdot t(t)$$

$$= \left[x_0 - \frac{mg}{q}(\mu\cos\alpha + \sin\alpha) - b\right]\cos\sqrt{\frac{q}{m}}\cdot t + \frac{mg}{q}(\mu\cos\alpha + \sin\alpha) + b \tag{16}$$

$$x(t) - \frac{mg}{q}(\mu\cos\alpha + \sin\alpha) - b = \left[x_0 - \frac{mg}{q}(\mu\cos\alpha + \sin\alpha) - b\right]\cos\sqrt{\frac{q}{m}}\cdot t \tag{17}$$

$$\cos\sqrt{\frac{q}{m}}\cdot t = \frac{x(t) - \frac{mg}{q}(\mu\cos\alpha + \sin\alpha) - b}{x_0 - \frac{mg}{q}(\mu\cos\alpha + \sin\alpha) - b}$$

$$t = \sqrt{\frac{m}{q}}\arccos\frac{x(t) - \frac{mg}{q}(\mu\cos\alpha + \sin\alpha) - b}{x_0 - \frac{mg}{q}(\mu\cos\alpha + \sin\alpha) - b} \tag{18}$$

By substituting Equation (13) and Equation (15) into Equation (11), we obtain Equation (16). This is the position equation. The velocity equation was obtained by differentiating the position equation. Using Equation (16), we obtained the time equation (t). The final output of the launch calculation was the magnitude of the initial velocity of the UAV when it took off from the launcher, using the derived equations for $v(t)$ and t.

Trajectory Prediction Calculation. The movement of the UAV (assuming the UAV has no motor or is just a dummy UAV) was assumed to resemble a parabolic motion, as shown in Figure 5(b). With reference to the kinematic equation of parabolic motion, the values of positions x and y can be obtained for each time unit.

$$x = x_0 + v_0\cos\theta t + at$$
$$y = y_0 + v_0\sin\theta t - 1/2gt^2 \tag{19}$$

The velocity on the x-axis still experienced acceleration under the concept of parabolic motion. The acceleration factor is required to modify the initial velocity. If there is no acceleration, the initial velocity will not change. Acceleration is obtained through a formula that satisfies Newton's Second Law in Equation (1). F represents the aircraft's thrust force, m is the aircraft's mass, and a is the acceleration. The calculation of the thrust value required peripheral parameters, namely the motor's angular speed (rpm), the diameter and pitch of the propeller, as well as the multiplication of motor power and efficiency factor. The magnitude of thrust was obtained through the equation formulated in the research.

$$F = p\frac{\pi(0.0254\cdot d)^2}{4}\left[\left(rpm\times 0.0254\times pitch\times\frac{1\text{ min}}{60\text{ s}}\right)2\right.$$
$$\left. - \left(rpm\times 0.0254\times pitch\times\frac{1\text{ min}}{60\text{ s}}\right)\times V_0\right]\times\left(\frac{d}{3.29546\times pitch}\right)1.5 \tag{20}$$

Because the magnitudes of thrust and mass were already known, the value of acceleration could be obtained. The next step was to determine the position and time of the turning points or reversal points. According to the concept of aerodynamics, for an aircraft to fly stably, the lift must be equal to the weight.

$$L = W \tag{21}$$

$$CL \cdot S \cdot \left(1/2 \cdot p \cdot v^2\right) = m \cdot g \tag{22}$$

S is the wing area of the aircraft, CL is the coefficient of lift force, p is the air pressure at a certain altitude (adopting the standard value of 1.225), and v is the velocity of the aircraft. The aircraft can fly upward and remain stable if the lift force exceeds its weight. Predicting the trajectory after passing the turning point significantly depends on the pilot's control, which complicates the estimation process. Based on this, trajectory prediction was limited until the UAV reached the turning point phase. After passing the turning point, the compiled trajectory prediction was based on general assumptions about a linear path involving regular increases in UAV altitude. This assumption relied on a constant climb angle of 25°.

5. **Results and Discussion.** Several experiments were conducted to evaluate the extent to which the design matched the realized outcomes. The main frame design of the UAV launcher was expected to have an inclination angle of approximately 10° and a launch frame length of approximately 350 cm. After the design realization process, it was found that the constructed UAV launcher had an exact inclination angle of 10° and a launch frame length of 340 cm. For this experiment, a UAV dummy was used, which was basically a UAV without propulsion and control systems. Testing was performed in manual mode using the push Up and Down buttons to control the DC motor and adjust the tension of the wire and cord to the desired level. The readings of tension values and launch angles were displayed on the TX system, and the results showed excellent performance. Wireless communication between the RX and TX systems could be safely conducted within a range of 2-5 m. Overall, the manual control function for operating the UAV launcher worked well and functioned smoothly. Next, testing of the automatic mode was conducted by using the push buttons SET1, SET2, and SET3. The testing with SET1 configuration involved the use of the DC motor with automatic winding function until the load cell sensor indicated a value of 20 kg, as programmed beforehand. Figure 6 shows the results of the UAV's movement during takeoff using SET1 tension (20 kg).

FIGURE 6. The UAV dummy executed takeoff with SET1 tension (20 kg)

The next experiment involved testing the SET2 and SET3 push button configurations. When either the SET2 or SET3 button was pressed, the DC motor would automatically wind the wire and bungee cord until the load cell sensor read values of 25 or 30 kg, which were displayed on the screen. Subsequently, when the trigger switch was activated, the UAV would take off with a trajectory similar to that of the previous SET1 testing.

5.1. **Testing of wingspan reading.** The test results shown in Table 1 indicated that the accuracy of the measurement box area readings was within the range of 94.08%. It could be concluded that the constructed measurement box was effective for predicting the UAV types.

TABLE 1. Testing of the measurement box with several objects

Object	Dimensions (m × m)	Real surface area (m^2)	Experimental surface area (m^2)	Accuracy (%)
1	0.158 × 0.248	0.039184	0.044052	87.58
2	0.104 × 0.23	0.023920	0.023967	99.80
3	0.147 × 0.213	0.313110	0.032600	95.88
4	0.280 × 0.325	0.091000	0.086886	95.47
5	0.207 × 0.289	0.059823	0.064796	91.68

5.2. **Launch testing.** In the testing with the UAV dummy, tests were conducted with different tension values as shown in Table 2. Because the dummy did not have a motor or internal power, it would inevitably fall, and the lowest point of its trajectory was the point of impact. To validate the accuracy of the trajectory prediction algorithm, we compared it with this data.

TABLE 2. Trajectory prediction testing with the UAV dummy using different tension values

Tension (kg)	Trajectory prediction falling point (m)	Falling point using a dummy UAV (m)	Error (m)
20	1.836	1.7	0.136
23.4	2.1981	1.92	0.2781
27	2.5838	2.6	0.0162

Data mapping point matching was conducted at intervals of 20 ms for each test. The data matching was precisely performed when the UAV took off or when it reached its highest point according to the altitude sensor readings.

Next, the same testing was conducted for tensions of 20 kg, 23.4 kg, and 27 kg as shown in Figure 7. Similar to the first flight, the data generated during the second flight tended to be unstable and exhibited considerable overshooting. This differed from the data produced by the simulation, which assumed ideal conditions. However, in the field, various external factors such as wind and other mechanical factors affected flight conditions. As a result, there was a discrepancy between the data generated by the altitude sensor and the overall readings. Even when testing with the same tension, the obtained data varied depending on the field conditions and launcher technical conditions. This difference indicated that the flight environment and conditions significantly affected the measurement results. After data processing and comparison, the error obtained was relatively small and not significantly different from the first testing (around 0.14 m).

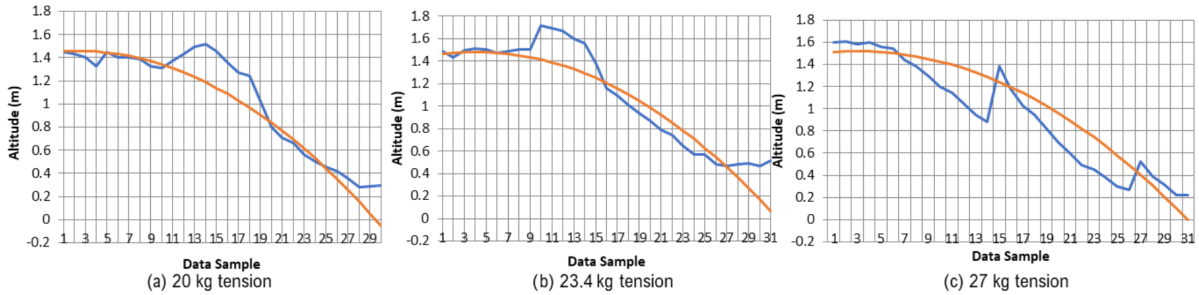

FIGURE 7. (color online) Comparison graph of trajectory prediction points (orange) with trajectory points of UAV dummy (blue) in the testing with (a) 20 kg, (b) 23.4 kg, and (c) 27 kg tension

Based on the testing results using the UAV dummy, it could be concluded that the system is capable of mapping the UAV's altitude position without the need for internal motor factors, and it performed well with a relatively small error.

5.3. **Trajectory prediction testing.** After conducting partial testing, the final step was to perform comprehensive system testing using an actual UAV. The specification of used UAV is shown in Table 3. Before conducting the trial, the UAV was placed inside the measurement box to obtain the wing area data as shown in Figure 8.

TABLE 3. UAV specifications

1.	UAV Dimensions		
	Wingspan length	1.4	m
	Body length	1.1	m
	Mass	1.4	kg
2.	Motor and Propeller		
	Number of motors	1	
	Total motor power	610	Watt
	Number of propellers	1	set
	Propeller dimensions	11 × 7	Inch
	Nominal Kv	1100	Kv

FIGURE 8. Measurement of wing area

In the testing stage, data regarding the UAV's wing area, was approximately ± 0.2006 m^2. In addition, information about the UAV specifications was gathered as shown in Table 3, such as a propeller diameter of 11 inches, propeller pitch of 7 inches, and motor angular

speed of 13200 rpm when using a 3 s battery or 12 V. The UAV's mass was recorded as 1.4 kg with a motor power of 610 W. These data were input into the simulation to perform UAV trajectory prediction. Unlike the UAV dummy, this UAV was equipped with a Pixhawk, which had an automatic data logging feature to record altitude at each time interval. This data was recorded in the form of logs with a 0.1-s interval. During the flight, altitude data were logged and accessed through the APM Planner apps. From the flight testing results, two primary data were obtained: flight status data and altitude data at each time point. The mobile device provided output in the form of an indicator light status corresponding to the trajectory results and the turning point altitude obtained from the simulation. Here are the simulation results from the three conducted flights and the output of mobile device. From the three trajectory prediction results shown in Table 4 and Figure 9, it is evident that the UAV managed to pass the turning point and flew

TABLE 4. The results of the UAV flight with different configurations

Experiment number	Number of bungee cords	Tension (kg)	Angle (°)	Real flight result	Simulation result	Mobile device results
1	2	28.4	9.7	Success	Success	Success
2	2	28.8	8.4	Success	Success	Success
3	2	30	8.2	Success	Success	Success

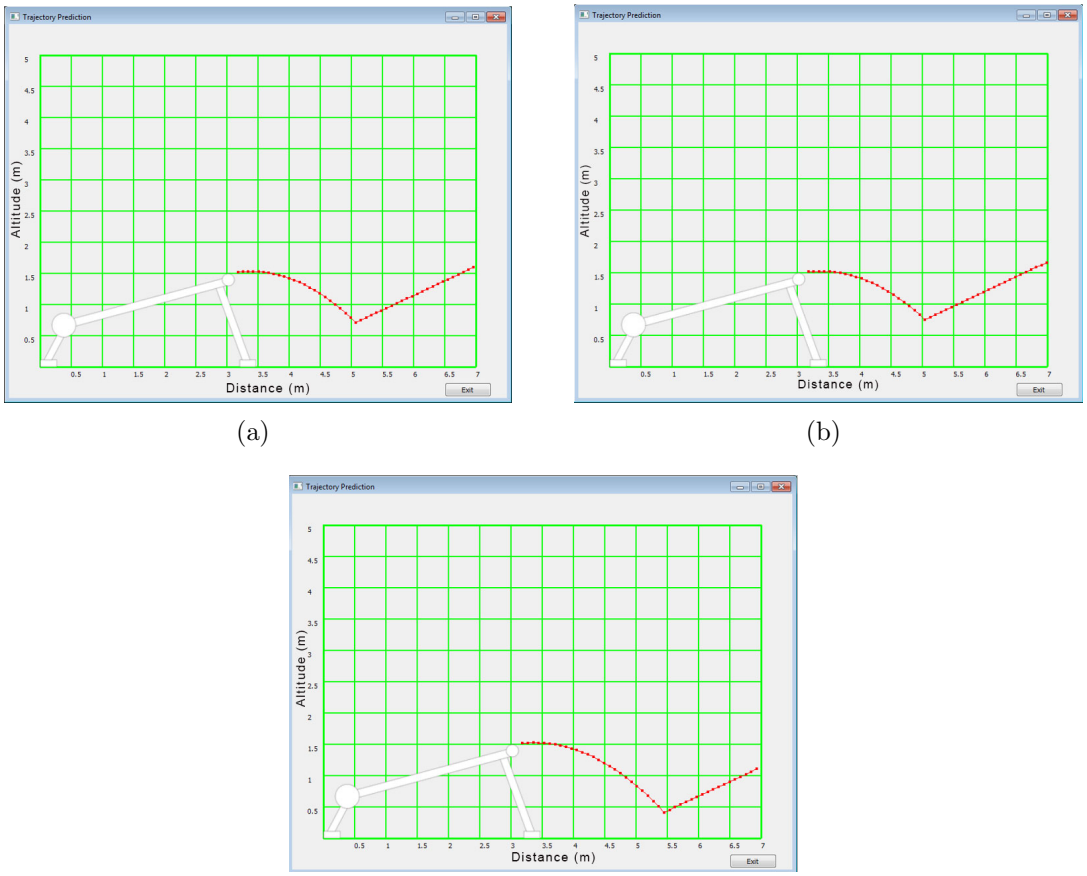

FIGURE 9. Trajectory prediction results of the (a) first flight with 28.4 kg tension, at the angle of 9.7°; (b) second flight with 28.8 kg tension at the angle of 8.4°; and (c) third flight with 30 kg tension at the angle of 8.2°

successfully, and the mobile device also provided the appropriate output. Next, a real-world test was conducted by flying the UAV following the same launcher configuration that was inputted in the simulation.

In terms of flight success, all tests did not encounter any failures and were consistent with the results from both the simulation and mobile device. However, due to limitations in testing altitude, only mobile device testing could be conducted to determine whether it was successful or not, but it could not validate the accuracy of the created indicators.

5.4. **Manufacturing costs.** Manufacturing costs using the Indonesian currency are shown in Table 5(A). The total manufacturing cost of the proposed UAV launcher is around $801.19. For the sake of comparison, the price of a commercially available UAV launcher in the market is shown in Table 5(B). It shows our launcher is cheapest compared to the competitors.

TABLE 5. List of parts and the manufacturing cost of the proposed UAV launcher compared to the other brands

(A)The proposed UAV launcher

Items	Price in IDR
Launcher frame set by a welder workshop	IDR 5,000,000
2 x Bungee Cord 12mm	IDR 300,000
Arduino Nano	IDR 50,000
Motor DC	IDR 1,300,000
Loadcell 50Kg	IDR 22,500
IMU GY521	IDR 17,900
2 x nRF24L01	IDR 46,000
VNH2SP30	IDR 97,500
LM2596	IDR 6,400
FlySky RC Remote Controller	IDR 710,000
Battery 2S	IDR 150,000
Battery 3S	IDR 240,000
Assembling Cost	IDR 5,000,000
Total	**IDR 12,940,300 ($801.19)**

(B)The proposed UAV launcher compared to other brands

Launcher Brand	Price (USD)
The proposed UAV Launcher	$ 801.19
UAV Catapult Launcher For Skywalker X8 Skywalker X5 Fixed-wing Aircrafts Airplane RTF PNP	$ 2,984.90
UAV catapult launcher For Skywalker X8	$ 153,760
L-80 UAV Catapult Launcher	$ 153,760
UAV Launcher Tl3 Nano	$ 8,000

5.5. **Limitations.** The launcher's performance has been tested in high-temperature environments. In hot temperatures (more than 35 degrees Celsius), direct sunlight will decrease the performance of the bungee cords. It will affect the bungee cord elasticity, so the launch power will decrease. To overcome this problem, please keep the launcher away from direct sunlight. Also, change the bungee cord regularly. The acceptable size of the fuselage UAV is up to 15 cm. It cannot be used for UAVs with propellers greater than 15 cm. It is only for small UAVs with a maximum weight of 2 kg.

5.6. **Safety procedure.** Safety procedures are required to prevent any accident as follows.

- All operators must wear a helmet as a head protector.
- Avoid staying behind the launcher to avoid accidents if the bungee cord is broken.
- Check all mechanical joins of the frame.
- Check the launcher stakes.
- Check the roller.
- Check the launcher support with the ground.

6. **Conclusions.** The automatic bungee cord-type UAV launcher has been successfully implemented. The pneumatic cylinder's use as a trigger system on the UAV launcher functions well, resulting in safer and easier operations. The automation process on the bungee cord-type UAV launcher works effectively, with the DC motor capable of winding the pull wire and bungee cord to the desired tension value. The vision-based UAV wing area prediction works well with accuracy of 94.08%. However, during overall system testing, external factors still affect the perfection of UAV takeoff. These factors include the use of dummy UAVs in testing and the influence of wind or weather conditions that can affect the UAVs performance during launch. The trajectory prediction simulation is capable of mapping altitude points with various parameters provided, primarily with different values of tension, angles, number of bungee cords, and UAV masses, yielding an average error of 0.1434 meters. Several mechanical and external factors of the UAV launcher affect the overall accuracy of the system, such as the jerking effect of the UAV due to the rocking cradle during the launching process and the influence of wind.

Acknowledgment. We would like to express our sincere gratitude to the Institut Teknologi Sepuluh Nopember (ITS) for their invaluable support throughout this research. We are also grateful to the Department of Electrical Engineering, Faculty of Intelligent Electrical and Informatics Technology, Institut Teknologi Sepuluh Nopember, for providing the necessary funding for this research. Their financial assistance has played a vital role in the successful completion of this research project.

REFERENCES

[1] A. Utsav, A. Abhishek, P. Suraj and R. K. Badhai, An IoT based UAV network for military applications, *2021 6th International Conference on Wireless Communications, Signal Processing and Networking (WiSPNET)*, Chennai, India, 2021.

[2] C. Liu, G. Wang, Y. Yan, C. Bao, Y. Sun and D. Fan, Pint-sized military UAV engine's tele-adjusting arm based on force feedback, *2010 2nd International Asia Conference on Informatics in Control, Automation and Robotics (CAR 2010)*, Wuhan, China, 2010.

[3] J. Xu, Q. Guo, L. Xiao, Z. Li and G. Zhang, Autonomous decision-making method for combat mission of UAV based on deep reinforcement learning, *2019 IEEE 4th Advanced Information Technology, Electronic and Automation Control Conference (IAEAC)*, Chengdu, China, 2019.

[4] T. H. Pham, D. Ichalal and S. Mammar, Complete coverage path planning for pests-ridden in precision agriculture using UAV, *2020 IEEE International Conference on Networking, Sensing and Control (ICNSC)*, Nanjing, China, 2020.

[5] S. Ghosh et al., Development of an IoT based robust architecture for environmental monitoring using UAV, *2019 IEEE 16th India Council International Conference (INDICON)*, Rajkot, India, 2019.

[6] X. Gu, T. Liu, D. Yang, K. Huang and Y. Tian, Research on application of maritime calibration based on fixed-wing UAV, *2019 IEEE 3rd Information Technology, Networking, Electronic and Automation Control Conference (ITNEC)*, Chengdu, China, 2019.

[7] D. Yin, X. Yang, H. Yu, S. Chen and C. Wang, An air-to-ground relay communication planning method for UAVs swarm applications, *IEEE Transactions on Intelligent Vehicles*, vol.8, no.4, pp.2983-2997, 2023.

[8] S. Wang, Y. Han, J. Chen, Z. Zhang, G. Wang and N. Du, A deep-learning-based sea search and rescue algorithm by UAV remote sensing, *2018 IEEE CSAA Guidance, Navigation and Control Conference (CGNCC)*, Xiamen, China, 2018.

[9] B. Yan and C. Wu, Research on taxi modeling and taking-off control for UAV, *2014 7th International Symposium on Computational Intelligence and Design*, Hangzhou, China, 2014.

[10] Y. Lu, Q. Chen, G. Jia and Z. Guo, Development and experiment of elastic-rope launcher for small fixed-wing UAVs, *2020 3rd World Conference on Mechanical Engineering and Intelligent Manufacturing (WCMEIM)*, Shanghai, China, 2020.

[11] Y. Leng, J. Xiao and B. Leng, Design of monitoring software of take-off and landing for UAV, *2016 International Conference on Network and Information Systems for Computers (ICNISC)*, Wuhan, China, 2016.

[12] P. Guruge, B. B. Kocer and E. Kayacan, A novel automatic UAV launcher design by using bluetooth low energy integrated electromagnetic releasing system, *2015 IEEE Region 10 Humanitarian Technology Conference (R10-HTC)*, Cebu, Philippines, 2015.
[13] A. S. Budiyanta, F. S. Pranoto, A. P. Adi and A. Wiyono, Design and testing of a bungee cord based launcher for LSU-02 UAV, *Journal of Industrial Research and Innovation*, vol.16, no.3, pp.114-120, 2022.
[14] K. Anuar, M. Akbar, W. Fatra, A. B. Priyofitrianto, T. Matua and H. A. Aziz, The design of bungee cord type launcher system for Serindit V-2 UAV, *The 2nd International Conference on Design, Energy, Materials and Manufacture (ICDEMM 2021)*, Pakanbaru, Indonesia, 2021.
[15] M. Huang, C. He and J. Pei, Dynamic analysis and optimization of pneumatic wedge-shaped launcher for UAV, *Transactions of Nanjing University of Aeronautics and Astronautics*, vol.35, no.5, pp.866-873, 2018.
[16] M. Kondratiuk and L. Ambroziak, Design and dynamics of kinetic launcher for unmanned aerial vehicles, *Applied Sciences*, vol.10, no.8, 2949, 2020.
[17] Y. Yu and W. Jun, Control strategies for the electromagnetic launcher for UAVs, *2015 34th Chinese Control Conference (CCC)*, Hangzhou, China, 2015.
[18] C. Liang, Z. Qiao, H. Xiang, X. Yuan, X. Zheng and Q. Lv, Overall technology research of an UAV-launcher system based on electromagnetic launch, *2020 3rd International Conference on Unmanned Systems (ICUS)*, Harbin, China, 2020.
[19] P. Thanghom, J. Pinyochon, P. Narathee, S. Weng and S. Surangsee, Spring drive UAV launcher, *Proceedings*, vol.39, no.1, DOI: 10.3390/proceedings2019039002, 2019.
[20] Z. Novakovic, Z. Vasic, I. Ilic, N. Medar and D. Stevanovic, Integration of tactical-medium range UAV and catapult launch system, *Scientific Technical Review*, vol.66, no.4, pp.22-28, 2016.
[21] Z. Novaković and N. Medar, Analysis of a UAV bungee cord launching device, *Scientific Technical Review*, vol.63, no.3, pp.41-47, 2013.

Author Biography

Ronny Mardiyanto received B.Eng. degree in Electrical Engineering from the Institut Teknologi Sepuluh Nopember (ITS), Indonesia, in 2003, M.Eng. degree in Electrical Engineering from the Institut Teknologi Bandung (ITB), Indonesia, in 2006, and Ph.D. degree from Saga University, Japan, in 2011. He is currently a lecturer at ITS. His current research interests include autonomous robot and artificial intelligent.

Devy Kuswidiastuti received B.Eng. degree in Electrical Engineering from the Institut Teknologi Sepuluh Nopember (ITS), Indonesia, in 2004, her M.Sc. degree from Hochschule Darmstadt, Germany, in 2008, and her Dr. degree from ITS in 2021. She worked in the Research and Development Engineering Department at Panasonic Shikoku Electronics, Indonesia, from 2004 to 2006. She is currently a lecturer at ITS. Her current research interests include MIMO radar and array signal processing.

Ruth Johana Hutagalung is a final-year Electrical Engineering student specializing in Electronics Engineering at Institut Teknologi Sepuluh Nopember, Indonesia. Her current research interests encompass the field of artificial intelligence.

Ahmad Fauzi Aulia finished his bachelor degree in 2019 on Institut Teknologi Sepuluh Nopember, majoring in Electronics. During his study, he took interests in analytical approach of various subjects, especially in developing an enhancement for existing product. He is currently working on PT Sumber Alfaria Trijaya as Service Measurement Specialist, specializing in data analysis.

Pradhipta Dwi Nugroho studied at the Indonesian Air Force Academy and graduated in 2012. He earned a bachelor's degree in Electrical Engineering from Institut Teknologi Sepuluh Nopember, Surabaya, in 2018. He now holds the rank of captain and works in the Indonesian Air Force as a radar technician and fighter controller. His current research interests include radar and fighter controller.